ORIGINAL RESEARCH

Myeloid-derived Suppressor Cells Are Necessary for Development of Pulmonary Hypertension

Andrew J. Bryant[1], Vinayak Shenoy[2], Chunhua Fu[1], George Marek[1], Kyle J. Lorentsen[1], Erica L. Herzog[3], Mark L. Brantly[1], Dorina Avram[1]*, and Edward W. Scott[4]*

[1]Division of Pulmonary, Critical Care, and Sleep Medicine, Department of Medicine, College of Medicine, University of Florida, Gainesville, Florida; [2]Department of Pharmaceutical and Biomedical Sciences, California Health Sciences University, Clovis, California; [3]Division of Pulmonary, Critical Care, and Sleep Medicine, Department of Medicine, Yale School of Medicine, New Haven, Connecticut; and [4]Department of Molecular Genetics and Microbiology, University of Florida, Gainesville, Florida

Abstract

Pulmonary hypertension (PH) complicates the care of patients with chronic lung disease, such as idiopathic pulmonary fibrosis (IPF), resulting in a significant increase in morbidity and mortality. Disease pathogenesis is orchestrated by unidentified myeloid-derived cells. We used murine models of PH and pulmonary fibrosis to study the role of circulating myeloid cells in disease pathogenesis and prevention. We administered clodronate liposomes to bleomycin-treated wild-type mice to induce pulmonary fibrosis and PH with a resulting increase in circulating bone marrow–derived cells. We discovered that a population of C-X-C motif chemokine receptor (CXCR) 2^+ myeloid-derived suppressor cells (MDSCs), granulocytic subset (G-MDSC), is associated with severe PH in mice. Pulmonary pressures worsened despite improvement in bleomycin-induced pulmonary fibrosis. PH was attenuated by CXCR2 inhibition, with antagonist SB 225002, through decreasing G-MDSC recruitment to the lung. Molecular and cellular analysis of clinical patient samples confirmed a role for elevated MDSCs in IPF and IPF with PH. These data show that MDSCs play a key role in PH pathogenesis and that G-MDSC trafficking to the lung, through chemokine receptor CXCR2, increases development of PH in multiple murine models. Furthermore, we demonstrate pathology similar to the preclinical models in IPF with lung and blood samples from patients with PH, suggesting a potential role for CXCR2 inhibitor use in this patient population. These findings are significant, as there are currently no approved disease-specific therapies for patients with PH complicating IPF.

Keywords: pulmonary hypertension; pulmonary fibrosis; myeloid-derived suppressor cell; C-X-C motif chemokine receptor 2; IL-8

Clinical Relevance

This study demonstrates for the first time that, in models of pulmonary hypertension, myeloid-derived suppressor cell trafficking to the lung, mediated by C-X-C motif chemokine receptor 2, is increased. Furthermore, a C-X-C motif chemokine receptor 2 antagonist inhibits granulocytic myeloid-derived suppressor cell accumulation within the lung, preventing development of PH.

(Received in original form June 7, 2017; accepted in final form August 20, 2017)

*D.A. and E.W.S. share senior co-authorship on this study.

This work was supported by the National Institutes of Health (NIH) grants KL2 TR001429 (A.J.B.) and P30 AG028740 (A.J.B.), the Gilead Sciences Research Scholars Program in Pulmonary Arterial Hypertension (A.J.B.), the Martha Q. Landenberger Research Foundation (A.J.B.), American Heart Association grants SDG12080302 (V.S.), R01 HL109233 (E.L.H.), and R01 AI067846 (D.A.), the University of Florida Gatorade Trust (D.A. and A.J.B.), and National Institute of Diabetes and Digestive and Kidney Diseases grant R01 DK105916 (E.W.S.).

Author Contributions: A.J.B. designed and performed experiments, analyzed data, and wrote the manuscript; V.S., C.F., G.M., and K.J.L. performed experiments; E.L.H. designed experiments and edited the manuscript; M.L.B. edited the manuscript; D.A. and E.W.S. designed experiments, analyzed data, and edited the manuscript.

Correspondence and requests for reprints should be addressed to Andrew J. Bryant, M.D., Department of Medicine, University of Florida College of Medicine, 1600 Southwest Archer Road, M-452, Gainesville, FL 32610-0225. E-mail: andrew.bryant@medicine.ufl.edu.

This article has a data supplement, which is accessible from this issue's table of contents at www.atsjournals.org.

Am J Respir Cell Mol Biol Vol 58, Iss 2, pp 170–180, Feb 2018

Originally Published in Press as DOI: 10.1165/rcmb.2017-0214OC on September 1, 2017
Internet address: www.atsjournals.org

Annual healthcare resource utilization for patients with idiopathic pulmonary fibrosis (IPF) costs greater than $2 billion dollars (1). Pulmonary hypertension (PH) associated with IPF is the most frequent comorbidity contributing to intensive use of hospital and emergency room services by this patient population (2, 3). Furthermore, IPF complicated by PH is associated with significant impairment in quality-of-life, and a fourfold increase risk of death (4, 5), compared with those patients with IPF alone. Despite the poor prognosis, there are currently no approved treatments for secondary PH. Vasodilator therapies have proven to be either unhelpful, or potentially harmful, when administered to patients with interstitial lung disease (6–8). Thus, there is a substantial need for novel and clinically translatable pharmacologic targets in the field of pulmonary vascular biology.

Our group and others have defined a role for myeloid-derived cells in the pathogenesis of PH (9, 10). Although the study of myeloid-derived cells in the pathobiology of vascular lung disease is still in its infancy, many groups have demonstrated strong evidence implicating leukocytes in the progression of PH (11, 12). Although, a vast number of immune effector cells are known to be involved in aberrant pulmonary vascular injury and repair (13–17), identification of a cellular intermediate orchestrating the response of these cells to inflammation and injury repair has remained elusive. Such an intermediary would prove to be a potentially efficacious drug target.

Previously, we have demonstrated the necessary role for chemokine receptors in the coordination of pathogenic vascular remodeling (18). Chemokine receptor C-X-C motif chemokine receptor (CXCR) 2 is an attractive focus for research in the field of vascular immunobiology (19), as it has been shown to be relevant to the pathogenesis of both PH (20) and pulmonary fibrosis (21). We therefore investigated whether examining CXCR2 in bleomycin-induced pulmonary fibrosis can help in identifying which cellular effectors are involved in PH development. We discovered that a progenitor myeloid-cell population, myeloid-derived suppressor cells (MDSCs), is necessary for the development of experimental PH, coordinating the inflammatory milieu contributing to pulmonary vascular remodeling. Moreover, we demonstrate that, by inhibiting CXCR2, pulmonary vascular changes are attenuated, through a decrease in pulmonary trafficking of a specific MDSC subset. Together, these data support analysis of CXCR2 inhibitors in this disease entity without currently available treatments.

Methods

Mice and Clodronate Depletion

All mice were wild type, on a C57BL/6 background, with equal numbers of male and females, aged 12–16 weeks (Jackson Laboratories). Myeloid cells were stimulated through induction of chronic macrophage apoptosis (22) with 100 μl intraperitoneal liposomal clodronate 1 week before either bleomycin or chronic hypoxia exposure, and every 3 days thereafter. Clodronate liposomes and control PBS liposomes were generated as previously described (23, 24). Animal experiments were conducted in accordance with the University of Florida (Gainesville, FL) Institutional Animal Care and Use Committee.

Bleomycin Model

Mice underwent intraperitoneal injection with 0.018 U/g bleomycin (Thermo Fisher Scientific) or vehicle twice weekly for 28 days (25, 26). Approximately 1 week after the last injection, 33 days after initiation of bleomycin, mice were harvested for histology and hemodynamic measurements.

CXCR2 Inhibition

The selective CXCR2 antagonist SB 225002 (1.5 mg/kg; Tocris Biosciences) or vehicle (1% DMSO in PBS) was injected

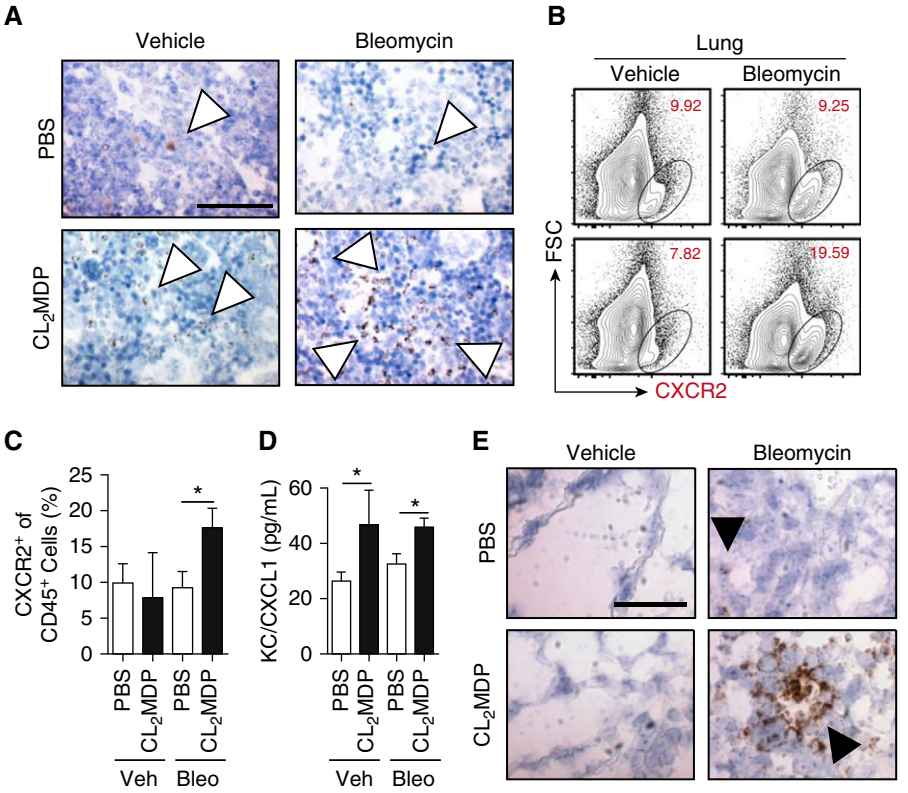

Figure 1. C-X-C motif chemokine receptor (CXCR) 2–expressing myeloid-derived cell expansion in macrophage-depleted, bleomycin-treated mice. (*A*) CXCR2 expression, by *in situ* hybridization (ISH), in the bone marrow (brown stain, open arrowheads) of mice that underwent 33-day intraperitoneal bleomycin protocol with either PBS or clodronate (CL_2MDP) liposome treatment. Scale bar: 100 μm, magnification ×60. (*B*) $CXCR2^+$ cells within the lung, analyzed by flow cytometry, (*C*) percentage gated on $CD45^+$ cells. (*D*) CXCL1 protein expression, assessed by multiplex array in whole mouse lung. (*E*) ISH of lung histology for CXCR2 expression (brown, solid arrowheads). Scale bar: 100 μm, magnification ×60 ($n = 12$ per mouse group over course of three independent experiments). Results are plotted as the mean (±SEM). *$P < 0.05$. Bleo = bleomycin; FSC = forward scatter; KC = CXCL1; Veh = vehicle.

intraperitoneally daily in mice (27), at initiation of the bleomycin protocol. Injections occurred throughout the 33-day bleomycin protocol.

Fibrosis Evaluation

Semiquantitative lung fibrosis scoring (28) and hydroxyproline microplate assay were performed, as previously described (29).

Hemodynamic Measurements

Invasive hemodynamic measurement was conducted, as described in previous studies (30). In brief, right ventricular (RV) systolic pressure (mm Hg) was assessed by right heart catheterization via the right internal jugular vein in spontaneously breathing anesthetized mice. Upon completion of the measurements, blood was collected. The heart was then excised with removal of the atria, and the RV and left ventricle (LV) plus septum were isolated for measurement of the RV:LV + S, as previously described (31).

Histologic Analysis

Upon harvest, the left lobe of the lung was inflated and placed in 10% formalin, as previously described (32, 33), and the right lobes were snap frozen in liquid nitrogen for RNA and protein processing. Immunostaining was performed for α-smooth muscle actin to identify muscularized pulmonary vessels, which were then counted per high-powered field, as previously described (34). Medial wall thickness was assessed using an established protocol (35). *In situ* hybridization for CXCR2 was performed per manufacturer instructions (Advanced Cell Diagnostics).

Antibodies and Flow Cytometry

All antibodies were used according to the manufacturer's recommended protocols. Flow cytometry analyses were performed on a BD LSR II or on FACSCalibur upgraded at three lasers and eight colors (Cytek). Data were analyzed using FlowJo software (Tree Star).

Proliferation Assay

T lymphocyte proliferation assay was performed as previously described (36).

Statistical Analysis

Statistical analysis was performed using GraphPad Prism 6.0 (GraphPad Software Inc.). Human data are presented as dot plots

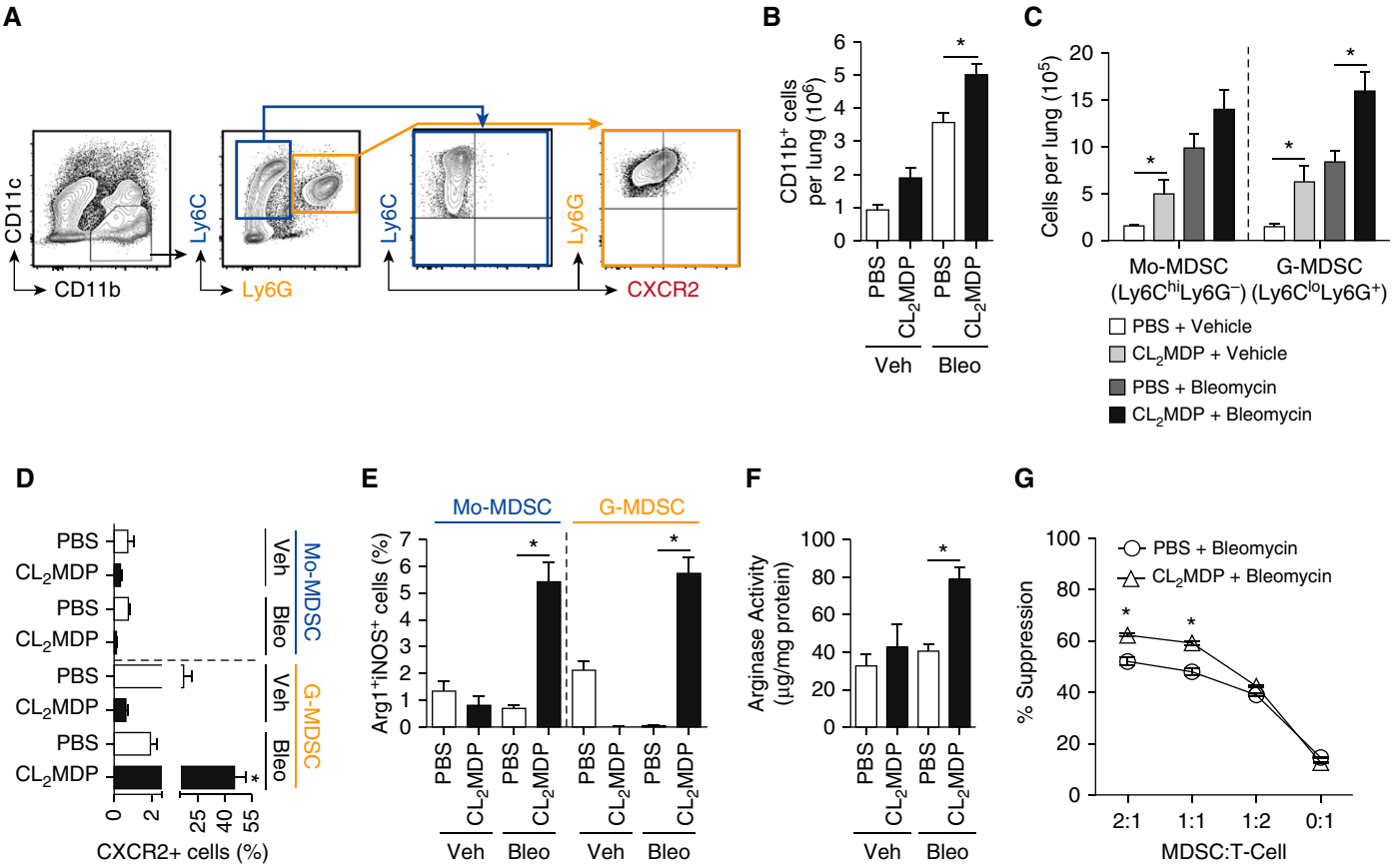

Figure 2. Infiltration of myeloid-derived suppressor cells (MDSCs) expressing CXCR2 into the lung in bleomycin treated mice with macrophage depletion. (*A*) Representative flow plot, where $CD11b^{+}Ly6C^{hi}Ly6G^{-}$ cells (highlighted in blue) represent monocytic MDSCs (Mo-MDSCs), and $CD11b^{+}Ly6C^{lo}Ly6G^{+}$ cells (highlighted in orange) represent granulocytic MDSCs (G-MDSCs). Gated on live singlet $CD45^{+}$ cells. (*B*) The absolute cell numbers of $CD11b^{+}$ cells, determined based on lung cellularity. (*C*) The absolute cell numbers of Mo-MDSC and G-MDSC of $CD11b^{+}$ cells based on lung cellularity. (*D*) The percentage $CXCR2^{+}$ cells of Mo-MDSC or G-MDSC cell population. (*E*) Percent arginase (Arg) 1^{+} inducible nitric oxide synthase (iNOS)$^{+}$ cells in Mo-MDSCs and G-MDSCs. (*F*) Whole-lung Arg activity of liposome-treated wild-type mice ($n = 12$ per group over course of three independent experiments). (*G*) $CD11b^{+}Gr\text{-}1^{+}$ cells were purified from the spleens of bleomycin- and liposome-treated mice and placed in a suppression assay with purified carboxyfluorescein succinimidyl ester–stained C57BL/6 T cells at the designated ratios. Anti-CD3/CD28 beads were used to induce proliferation. Cells were harvested on Day 5 and analyzed by flow cytometry for dilution ($n = 8$ per mouse group experiment). Results are plotted as the mean (±SEM). *$P < 0.05$. Ly6 = lymphocyte antigen 6 complex.

of median and interquartile range. Data were compared using ANOVA with Bonferroni post-test for multiple comparisons or the nonparametric two-tailed Mann-Whitney test, as appropriate. Mouse data are expressed as means (±SEM). As appropriate, groups were compared by ANOVA; follow-up comparisons between groups were conducted using Student's *t* test. A *P* value of 0.05 or less was considered to be significant. Please *see* the data supplement for more details. Of note, portions of this article have been previously published in abstract form (37).

Results

CXCR2 Expression Is Increased in Pulmonary Fibrosis

Mice do not naturally develop changes consistent with either PH or IPF. However, intraperitoneally administered bleomycin is a validated model for study of immune cells in pulmonary fibrosis (25), yielding a significant and consistent degree of vascular remodeling (9, 26). To this end, we treated wild-type C57BL/6 mice with bleomycin (0.018 U/g mouse) twice weekly for 4 weeks, followed by a 5-day observation period, before harvest and collection of tissue for analysis. To determine the pulmonary inflammatory response to an increase in the number of circulating myeloid cells (38), we concurrently dosed mice with twice-weekly clodronate liposomes (100 μg/injection) beginning 1 week before initiation of the bleomycin treatment and continuing until the day they were killed. Using these techniques, we found that overall bone marrow cellular CXCR2 expression was increased in the clodronate liposome–treated group compared with the PBS liposome controls (Figure 1A). This staining correlated with an increased percentage of $CXCR2^+$ leukocytes, analyzed by flow

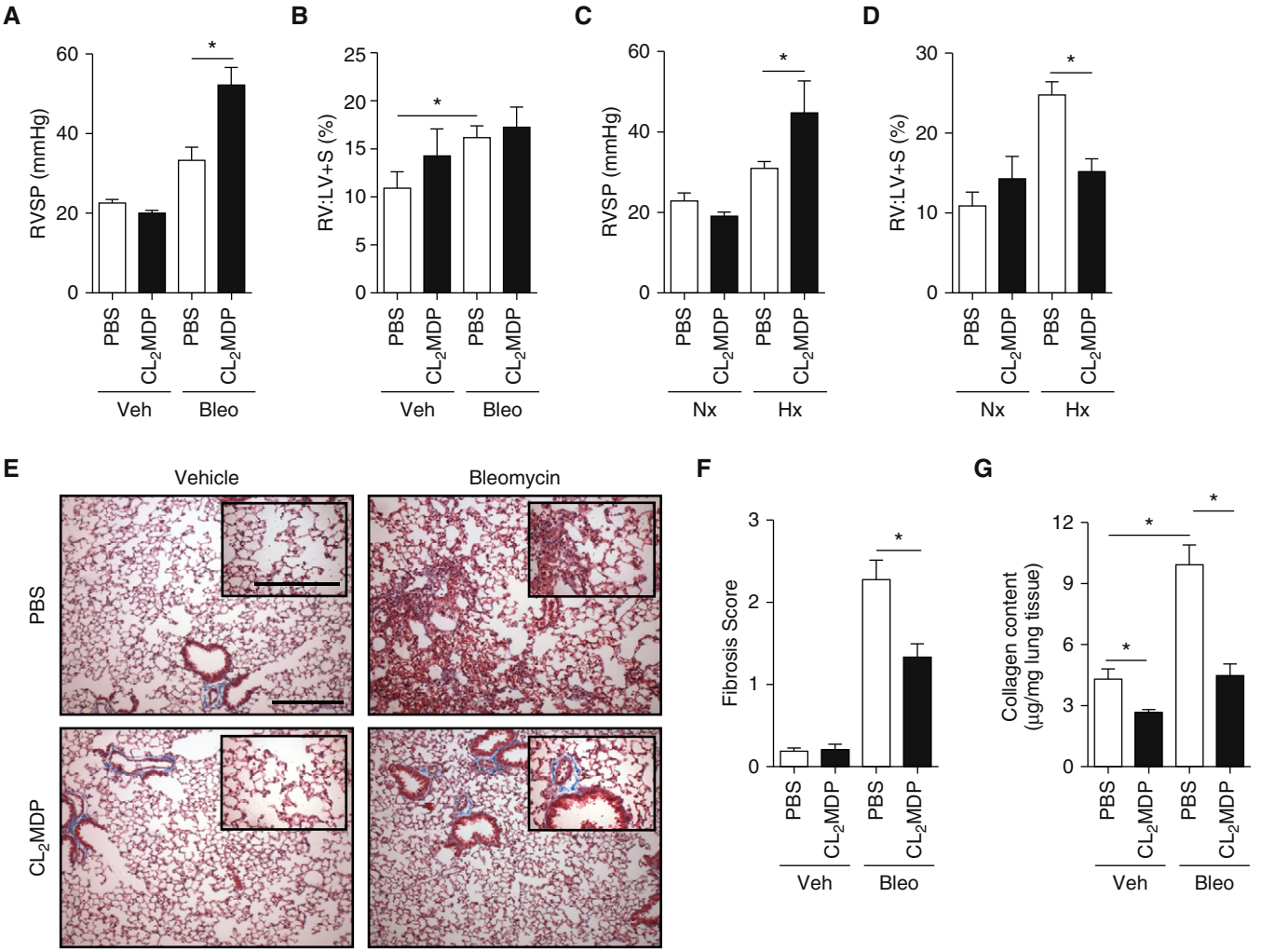

Figure 3. Effect of G-MDSC accumulation on pulmonary hypertension (PH) and fibrosis. (*A*) Right ventricular (RV) systolic pressure (RVSP) was assessed by invasive catheterization of the internal jugular vein on mice on Day 33 of the bleomycin protocol. (*B*) RV remodeling was assessed at time of death by RV to left ventricle (LV) plus septum mass (RV:LV+S) percentage. (*C*) RVSP and (*D*) RV:LV + S were assessed in mice treated with liposome preparations beginning 1 week before, and continuing throughout, the chronic hypoxia protocol (FI_{O_2}, 10% exposure for 28 d). (*E* and *F*) Pulmonary fibrosis was assessed using modified Ashcroft (fibrosis) score, averaging 10 random high-powered fields of Masson trichrome–stained lung sections, at ×20 magnification. Magnification ×10 and ×20 (inset). Scale bars: 500 μm and 200 μm (inset). (*G*) Collagen content was determined using standard hydroxyproline assay ($n = 12$ per mouse group over course of three independent experiments). Results are plotted as the mean (±SEM). *$P < 0.05$. Hx = hypoxia; Nx = normoxia.

cytometry ($CD45^+$ gate), from the lung of clodronate/bleomycin–treated mice (Figures 1B and 1C). Finally, we found an increase in whole-lung chemokine CXCL1 (the primary murine CXCR2 ligand, assessed by multiplex array; Figure 1D) in clodronate-treated compared with PBS-treated bleomycin mice. From these data, we concluded that bleomycin and clodronate liposome exposure plausibly increases in $CXCR2^+$ cell trafficking to the lung.

To gain insight into effector cell distribution, we examined lung histology for localization of CXCR2. Although the chemokine receptor was only mildly expressed in bleomycin- and PBS-treated mouse sections, there was a substantial increase in the number of $CXCR2^+$ cells in the clodronate groups (Figure 1E). Strikingly, CXCR2 was expressed most strongly around pulmonary vessels. These data suggest that CXCR2-expressing cells may help coordinate pulmonary vascular inflammatory changes.

Granulocytic MDSC Trafficking Is Increased in Pulmonary Fibrosis

CXCR2 can decorate many different populations of myeloid cells, such as mature neutrophils and MDSCs. MDSCs, however, are known to play a role in not only pulmonary bleomycin-induced injury (39), but infectious/inflammatory lung disease as well (40, 41). Broadly, MDSCs can be divided into subpopulations either morphologically or phenotypically, morphologically similar to monocytes (monocytic MDSC [Mo-MDSC], $CD11b^+Ly6C^{hi}Ly6G^-$) or granulocytes (granulocytic MDSC [G-MDSC], $CD11b^+Ly6C^{lo}Ly6G^+$). Of note, chronic administration of clodronate liposomes has previously been shown to increase tissue levels of MDSCs in models of chronic inflammatory stimulation (42, 43). Because G-MDSCs express high levels of CXCR2 (44, 45), we next sought to evaluate these cells in lungs of bleomycin-clodronate mice. As expected, clodronate and bleomycin administration resulted in an increase in whole-lung $CD11b^+$ cells (Figures 2A and 2B). Of these cells, G-MDSCs, but not Mo-MDSCs, were increased in the bleomycin- and clodronate-treated groups compared with bleomycin and PBS liposome controls (Figure 2C). In addition, percentage of $CXCR2^+$ cells was nearly 80-fold higher in G-MDSCs analyzed from mice treated with both bleomycin and clodronate liposome compared with those with bleomycin and PBS control (Figure 2D). These data support our hypothesis that G-MDSC accumulation within the lung is associated with increased CXCR2 expression.

G-MDSCs Accumulated in the Fibrotic Lung Express Arginase 1 and Inducible Nitric Oxide Synthase

MDSCs mediate tumor cell immune escape through arginine substrate sequestration and metabolism, via dual expression of arginase (Arg) 1 and inducible nitric oxide synthase (iNOS) (46). Expression of these enzymes by MDSCs in PH is unknown. Therefore, we analyzed the MDSC subpopulations for $Arg1^+iNOS^+$ expression. We found that G-MDSCs from bleomycin-treated mice expressed higher levels of Arg1 and iNOS than the vehicle-treated controls (*see* Figure E1A in the data supplement; Figure 2E). We next demonstrated whole-lung increase in Arg activity (Figure 2F) in bleomycin-clodronate–treated animals, consistent with the flow data, although nonspecific for Arg1. Finally, we confirmed isolated MDSC's immune suppressive capability in a T cell suppression assay (36). Consistent with the enzymatic expression data, we found that MDSCs, isolated from bleomycin and clodronate liposome–treated mice spleen, functionally suppressed *in vitro* T cell growth (Figure 2G). Importantly,

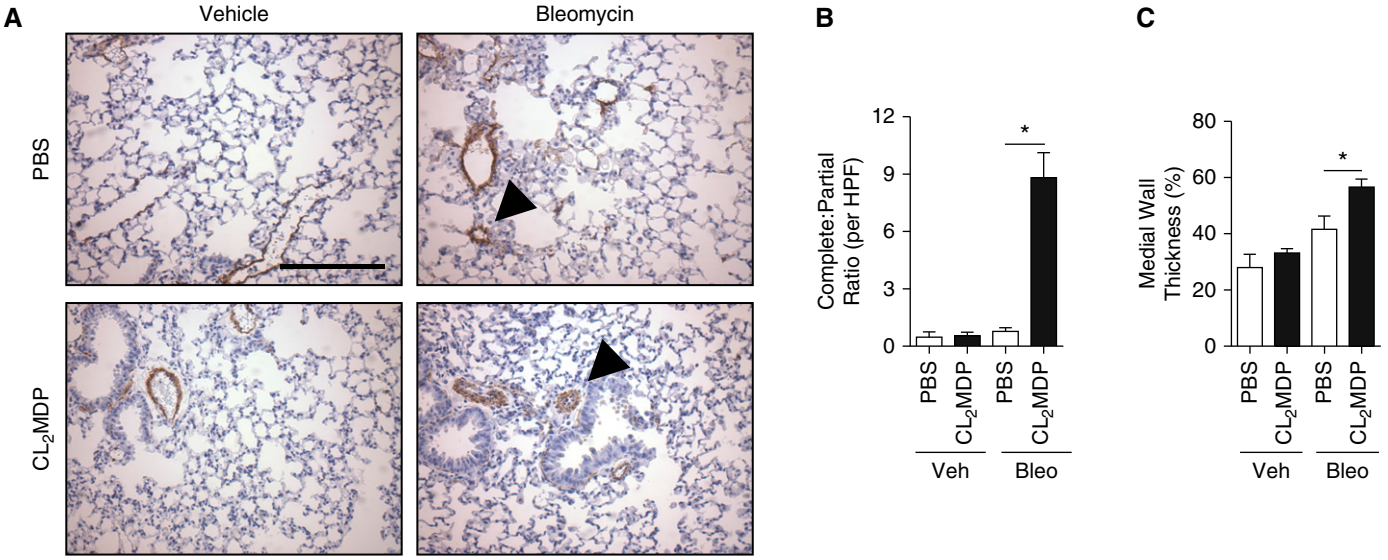

Figure 4. G-MDSC–associated effect on vascular remodeling in PH. (*A*) Immunohistochemical (IHC) staining for α-smooth muscle actin (α-SMA; brown, arrowheads) of lung sections from bleomycin-exposed mice, collected at time of time of death. Scale bar: 500 μm, magnification ×20. (*B*) Complete and partially muscularized vessels were counted from 10 microscopic fields and ratio calculated. (*C*) Medial wall thickness of pulmonary vessels was assessed by averaging from 10 random high-powered fields, opposing wall thickness of vessel (W1 and W2), in ratio to total diameter (d) (d = ([W1 + W2] / d) × 100%); $n = 12$ per mouse group over course of three independent experiments. Results are plotted as the mean (±SEM). $^*P < 0.05$. HPF = high power field.

spleen-derived MDSCs grossly reflected the same CXCR2, Arg1, and iNOS expression pattern as that of those analyzed from the lung of treated animals (Figures E1B and E1C). Finally, whole-lung expression of G-MDSC–associated growth factors, such as vascular endothelial growth factor and granulocyte-colony–stimulating factor, and remodeling protein matrix metallopeptidase 9, were increased in bleomycin and clodronate liposome–treated animals, compared with appropriate controls (Figures E1D and E1E). Together, these data support that MDSC trafficking to the lung is increased, and that these cells retain functional immunosuppressive function.

CXCR2-Expressing G-MDSCs Are Associated with Development of PH in Absence of Pulmonary Fibrosis

Clodronate liposomes administered in models of pulmonary vascular disease (47) have variable effects (48). Similar heterogeneity in response to clodronate treatment is described in the pulmonary fibrosis literature (23), dependent mainly upon early or late administration relative to bleomycin exposure (49). We therefore sought to define in the bleomycin model, administered either clodronate or PBS liposomes, the PH and fibrosis phenotype. We subsequently found a large increase in PH without evidence of RV hypertrophy by RV to LV plus septal mass ratio (RV:LV + S; %) in mice treated with bleomycin and clodronate (Figures 3A and 3B). In addition, we demonstrated the same physiologic findings in chronic hypoxia (F_{IO_2} 10% exposure, at normal atmospheric pressure, for 4 wk) induced PH (Figures 3C and 3D). Pulmonary vascular pressures were increased, despite a marked decrease in parenchymal fibrosis, as assessed by fibrosis score (Figures 3E and 3F) and measurement of collagen content (Figure 3G). From these findings, we conclude that, despite an improvement in pulmonary fibrosis, PH is worsened, associated with MDSC trafficking into the lung.

G-MDSC–associated Vascular Remodeling Contributes to PH

MDSCs accelerate angiogenesis, metastasis, and vascular injury and repair (50, 51). Therefore, we examined lung sections from

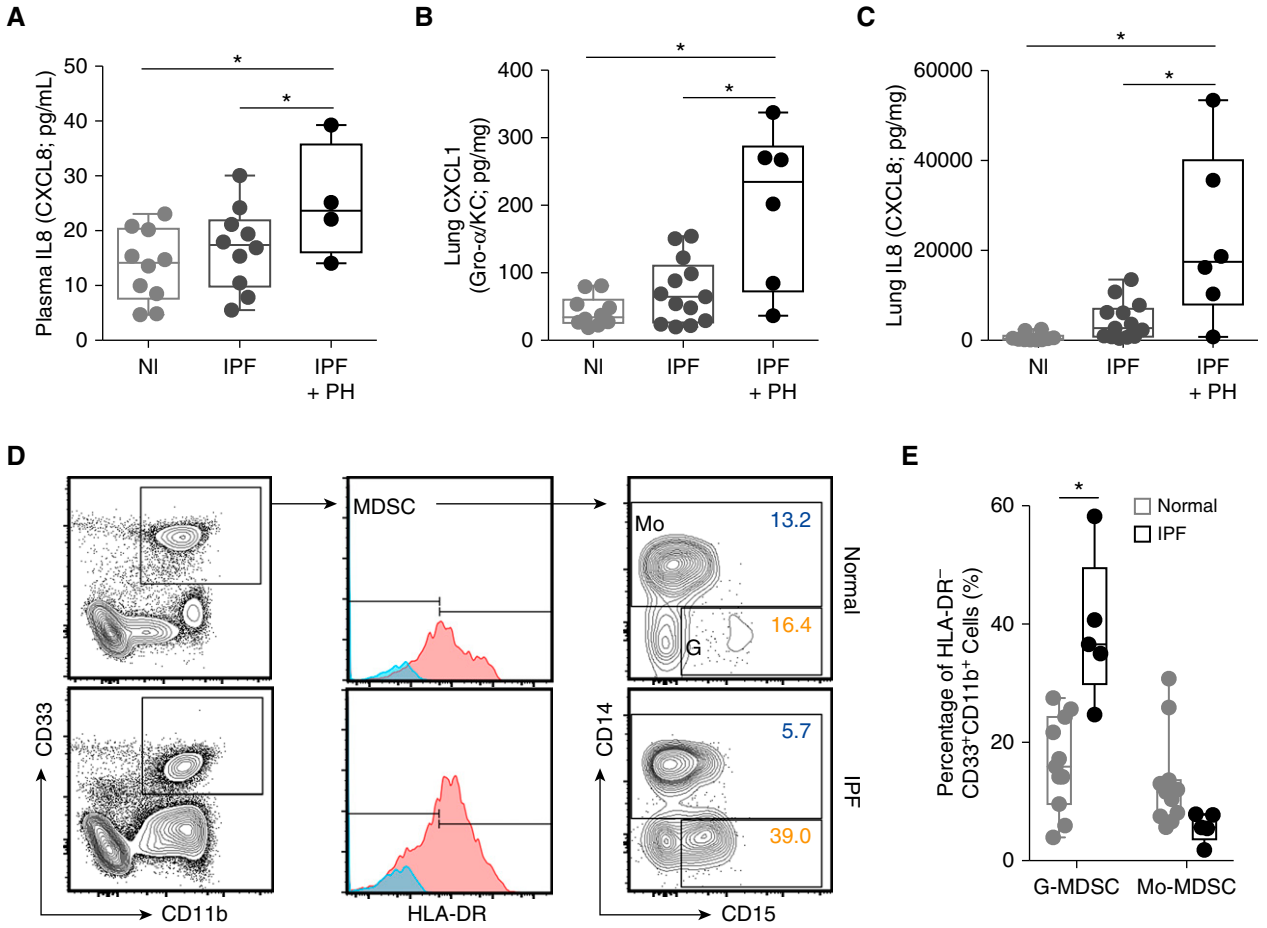

Figure 5. CXCR2 signaling and circulating G-MDSCs in patients with, or at risk for development of, PH associated with idiopathic pulmonary fibrosis (IPF). (*A*) Plasma IL-8 (or CXCL8) from normal (NI; $n = 10$) control subjects and patients with IPF with ($n = 4$) and without ($n = 10$) PH, as analyzed by multiplex array. (*B*) Whole-lung tissue CXCL1 and (*C*) IL-8, evaluated by multiplex array, from samples from NI patients ($n = 10$), patients with IPF alone ($n = 13$), and patients with IPF with PH ($n = 6$). (*D*) Representative flow plots for determination of $CD11b^+CD33^+HLA\text{-}DR^-CD14^-CD15^+$ cells (human G-MDSC) and $CD11b^+CD33^+HLA\text{-}DR^-CD14^+$ cells (human Mo-MDSC) from the peripheral blood of patients with IPF ($n = 5$) versus healthy control subjects ($n = 11$). Boxes represent the interquartile range, and the horizontal lines are the medians. *$P < 0.05$. HLA-DR = human leukocyte antigen–antigen D related.

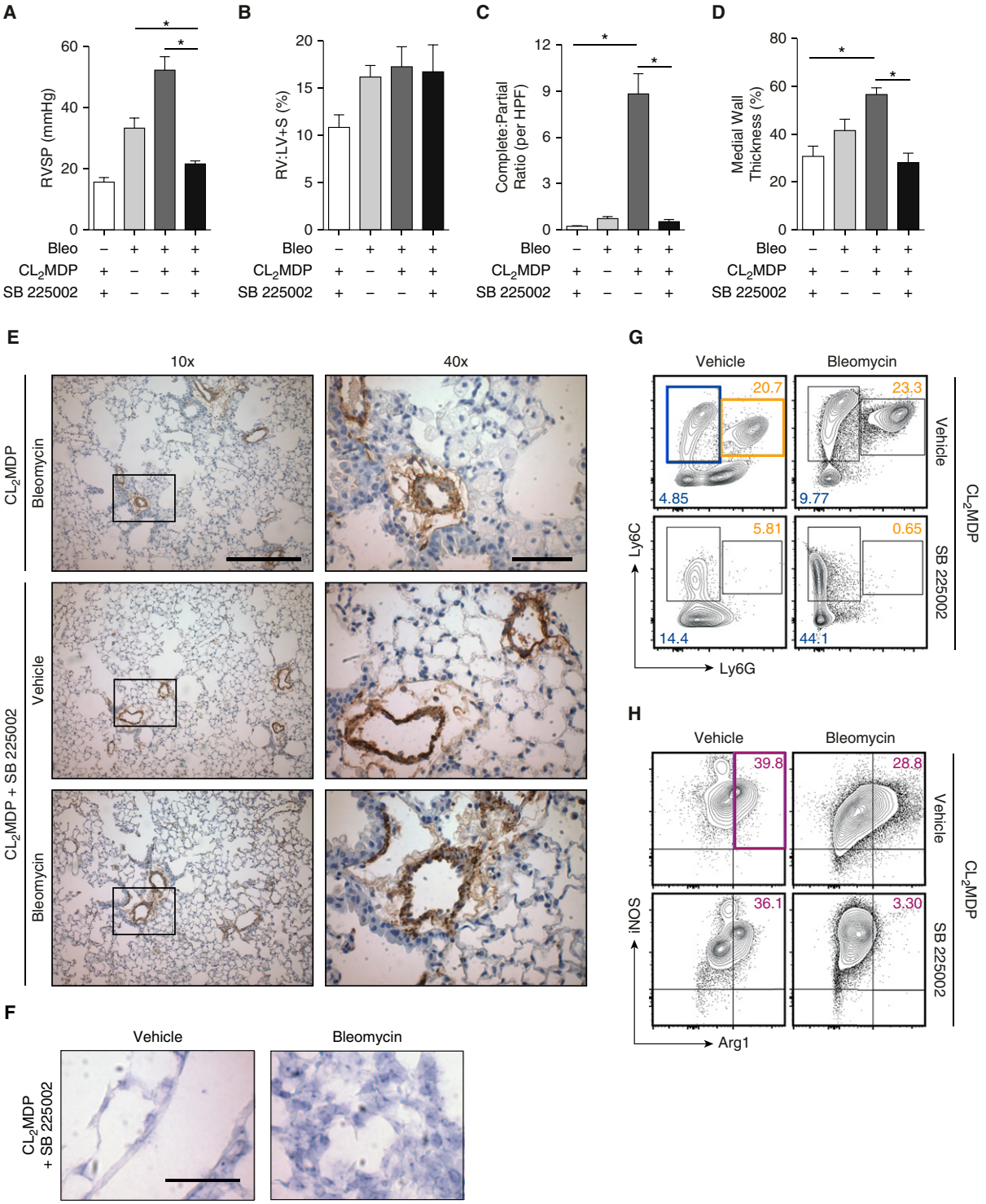

Figure 6. Effect of CXCR2 inhibition on PH, vascular remodeling, and G-MDSC accumulation within the lung. (*A*) RVSP was assessed in mice treated with bleomycin, CL_2MDP liposomes, and CXCR2 inhibitor SB 225002. (*B*) RV remodeling was assessed at time of death, by RV:LV + S percentage. (*C*) Complete and partially muscularized vessels were counted from 10 microscopic fields, and the ratio was calculated. (*D*) Medial wall thickness of pulmonary vessels was assessed by averaging from 10 random high-powered fields. (*E*) α-SMA IHC staining of lung sections from treated mice. Scale bars: 500 μm (×10) and 100 μm (×40). (*F*) *In situ* hybridization lung histology for CXCR2 expression. Scale bar: 100 μm, magnification ×60. (*G*) Representative plots of Mo-MDSCs (blue highlight) and G-MDSCs (orange highlight) from whole lungs in treated mice. (*H*) Representative plots (gated on total MDSCs, given low levels of cellularity in G-MDSC population) of whole-lung Arg^+iNOS^+ cells (purple highlight). (*I*) The percentage Mo-MDSC and G-MDSC of $CD11b^+$ cells. (*J*) The percentage Arg^+iNOS^+ cells of total MDSCs ($n = 6$ per mouse group experiment). Results are plotted as the mean (±SEM). $^*P < 0.05$.

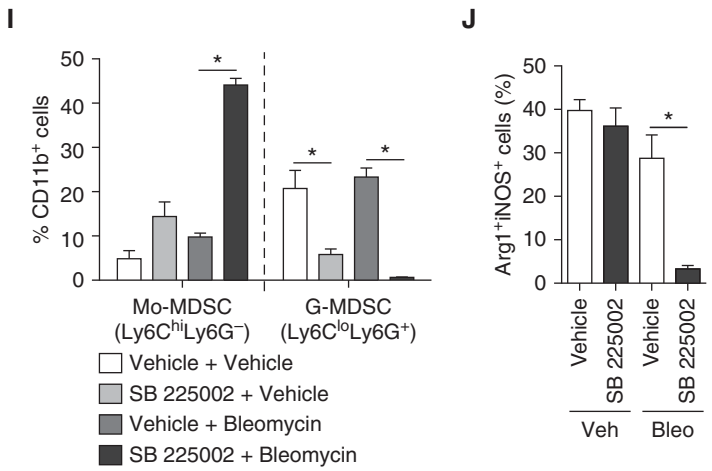

Figure 6. (Continued).

the clodronate- and bleomycin-treated mice for evidence of vascular remodeling by pulmonary vessel muscularization counts (52). Though number of muscularized pulmonary vessels was similar between PBS- and clodronate liposome–treated bleomycin-exposed mice (data not shown), complete (circumferential) muscularization was nearly ninefold higher in the clodronate group. These changes were associated with an increase in medial wall thickness by greater than 10% (Figures 4A–4C). These data support a contributory role of G-MDSCs, expressing CXCR2, in vascular remodeling that leads to PH.

PH Associated with IPF Parallels Preclinical Studies

We next sought to understand if an MDSC population was present in patients with disease. Unlike mice, in humans, the major ligands for CXCR2 are CXCL8 (also known as IL-8) and, to a lesser extent, CXCL1 (36). CXCL8 has previously been linked to the pathogenesis of both IPF (53) and PH (54, 55). Therefore, we first tested plasma samples, from the National Institutes of Health Lung Tissue Research Consortium cohort, and found a significantly higher level of CXCL8 in patients with IPF and PH compared with normal control subjects or patients with IPF alone (Figure 5A). Levels of CXCL1 and CXCL8 in lung homogenates from the samples from patient with IPF and PH were likewise elevated compared with disease control samples from patient with IPF alone (Figures 5B and 5C).

To explore whether patients with IPF have a greater circulating amount of G-MDSCs compared with nondisease control subjects, we prospectively recruited both normal control subjects ($n = 11$) and patients with a diagnosis of IPF ($n = 5$) from the University of Florida Pulmonary Interstitial Lung Disease Clinic (Gainesville, FL) (patient characteristics, Table E1). All patients that carried a diagnosis of IPF were on antifibrotic therapy (single or dual agent), though none were currently on vasodilator therapy. The peripheral blood G-MDSC population in patients with IPF was double that of normal control subjects (Figures 5D and 5E; median and interquartile range presented), with no significant difference noted in Mo-MDSCs. These data demonstrate that the chemokine axis shown to be essential for MDSC recruitment in murine PH development is also active in patients with IPF and PH, and the specific G-MDSC population is at least elevated in patients with IPF versus healthy control subjects.

PH Is Prevented through Blockade of G-MDSC Trafficking to the Lung by CXCR2 Inhibitor

Previously, CXCR2 inhibition has been shown to be important in experimental development of both PH (19, 20) and pulmonary fibrosis (56), although a mechanism remains unspecified. Because $CXCR2^+$ G-MDSCs are abundant and strongly associated with PH, we hypothesized that blocking CXCR2 could prevent G-MDSC recruitment and attenuate the phenotype. Therefore, we chose to study antagonism of CXCR2 in the bleomycin-clodronate model of PH through use of small molecular inhibitor, SB 225002 (daily intraperitoneal injection of 1.5 mg/kg mouse), initiated at the start of the bleomycin protocol. In mice administered SB 225002, PH was completely attenuated with resolution of pulmonary vessel muscularization to that of a normal wild-type control (Figures 6A–6E), with complete absence of perivascular CXCR2 expression (Figure 6F). CXCR1 expression was unchanged in SB 225002-treated mice compared with controls (Figure E3A). Consistent with the literature (21), the percentage of granulocytes in the lung, after treatment with CXCR2 inhibitor actually trended toward being higher compared with control mice, arguing that neutrophil depletion in the model does not account for the phenotype (Figure E3B). The lack of CXCR2 expression within the lung and the resolution of the pulmonary vascular phenotype correlated directly with decreased infiltration of G-MDSCs (Figure 6G), and a corresponding increase in Mo-MDSCs in mice given SB 225002, clodronate liposome, and bleomycin compared with controls. In the complete MDSC population, dual-positive $Arg1^+iNOS^+$ cell populations were nearly absent in mice given SB 225002 in the bleomycin and clodronate liposome group (Figures 6H–6J), suggesting a comprehensive decrease in functional capability of these cells. These results demonstrate that CXCR2-mediated recruitment of G-MDSCs is necessary for development of PH.

Altogether, our data implicate G-MDSCs in the pathophysiology of PH (with the proposed mechanism summarized in Figure 7). Identification of these cells offers a translatable and therapeutic option to improve patient outcomes by targeting the CXCR2-positive subset of MDSCs. Though our work demonstrates utility in only prophylaxis against development of PH—as opposed to treatment of existing vasculopathy—we have demonstrated a plausible biologic mechanism for disease, laying the groundwork for performance of a clinical trial of CXCR2 inhibitors in this patient population without any current therapies.

Discussion

We present data that show that G-MDSCs expressing CXCR2 can cause PH in a model of pulmonary fibrosis, despite improvement in parenchymal lung disease. Functional and expression analysis showed that MDSCs retained immunosuppressive capabilities in these models. In addition, we demonstrate human pathology consistent with the

preclinical studies in patients with IPF. Finally, the murine pulmonary vascular disease is completely attenuated by antagonizing CXCR2-mediated trafficking of G-MDSCs.

MDSCs evolved as a response to inflammatory stimuli, likely to minimize collateral tissue damage inflicted during the immune response to infection. However, in the setting of chronic inflammatory stimulus, this same cell population can induce a state of immune senescence, facilitating unchecked aberrant cellular proliferation (57, 58). This malignant effect has fostered development of MDSC-inhibiting strategies, including agents directed at cell deactivation (phosphodiesterase-5 inhibitors [59]), differentiation (all-trans retinoic acid [60]), and multikinase inhibitors (61), which block cell development. Acting in a synergistic fashion with novel immunotherapeutic agents directed against, for example, programmed cell death protein 1 (36), CXCR2 inhibitors have shown promising results in impeding MDSC movement and function. Importantly, CXCR2 antagonists are currently being studied in patients with severe chronic obstructive pulmonary disease, having been proven to be both safe and efficacious in phase II clinical trials (62). Our study provides solid preclinical evidence for further study of CXCR2 inhibitors in prevention, and potentially treatment, of PH associated with IPF.

Circulating MDSCs are upregulated in children with PH (63), and in patients with IPF (64). In patients with IPF, $CD33^{+}CD11b^{+}$ cells, consistent with an MDSC expression pattern, are found within the fibrotic niche of fibrotic lung sections. Given these data and our own, it is intriguing to speculate on the use of MDSC subpopulations in identifying patients for either clinical trial enrollment, or, eventually, as informing therapeutic intervention decisions.

Although our work does not define the downstream mechanism of MDSC-mediated pulmonary vascular changes, inferences for future studies can be drawn from the demonstrated immune suppression data, specifically pertaining to arginine substrate utilization. Arginine metabolism coordinated by MDSCs through the enzymes, Arg1 and iNOS, plays many important roles in the immune suppression capability of MDSCs. Arg1 in particular leads to dysfunction of T cells through blocking the main signaling component of the T cell receptor, while simultaneously producing increased amounts of proline necessary for collagen formation (65). Related to malignant stroma fibrotic remodeling, G-MDSCs are the primary source of Arg1 in tumor-bearing hosts, acting as the major basis of extracellular arginine depletion (66).

A limitation of our study is that it is underpowered to detect a difference in the MDSC population within our samples from patients with IPF. In future studies with larger patient recruitment, attention will be paid to appropriate age and tobacco smoke exposure matching between healthy control subjects and patients with disease. Likewise, it is worth noting that, in the aforementioned study of MDSCs in patients with IPF, the authors described an opposite finding from our own limited report. Specifically, the group noted that, in their patients with IPF, Mo-MDSCs were elevated, whereas G-MDSCs were unchanged compared with control subjects (64). This discrepancy in MDSC subpopulations may have been due to a number factors, including differences in flow cytometric analysis, or the fact that all of our patients with IPF were receiving concurrent antifibrotic therapies. The tyrosine kinase inhibitor family of therapeutics, of which the drug, nintedanib, is currently approved for treatment of interstitial lung disease, are known to alter maturation and function of MDSCs, resulting in multiple cytotoxic T cell changes. Given that G-MDSCs function predominantly as an antigen-specific T lymphocyte–suppressive agent, distinction between MDSC subgroup response to therapies has potentially important implications for treating patients with concurrent PH (67, 68).

In total, other leukocytes far outnumber MDSCs within the lung, with multiple redundant regulatory pathways operating to decrease pathologic signaling (69–71). However, little is known about these regulatory networks related to the pulmonary vasculature. Complexity of regulation highlights the potential negative outcomes of broadly directed immunobiologic targeted therapy (72). A rigorous approach is required for use of adjuvant therapies, especially with application to disease entities outside the scope of cancer treatment. CXCR2 inhibitors are a class of drugs that has been shown to be safe in patients with advanced lung disease. Therefore, this class of drugs should be considered in clinical trials of patients with IPF at risk for development of pulmonary vascular disease. ■

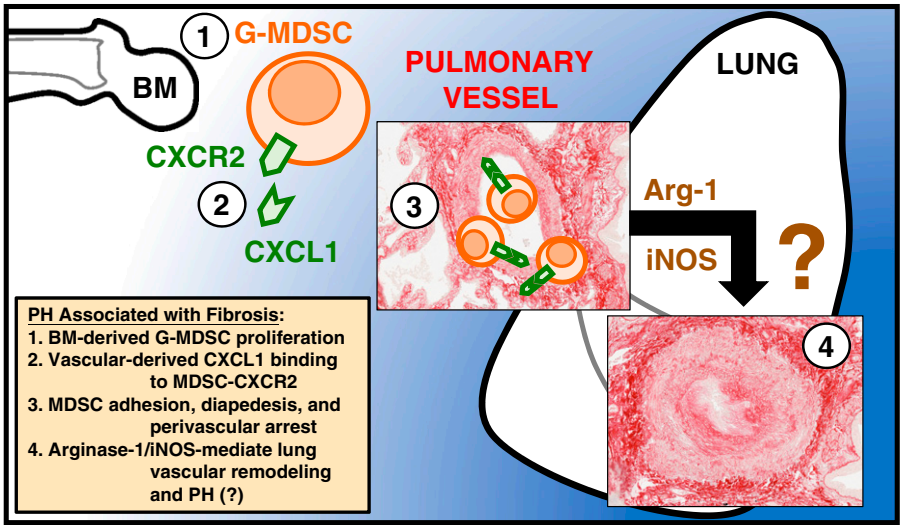

Figure 7. Model illustrating how G-MDSC trafficking contributes to PH through CXCR2. (*1*) Induction of bone marrow (BM) proliferation and release of G-MDSCs into circulation. (*2*) G-MDSC–expressed CXCR2 binds vascular endothelium–derived ligand, CXCL1 (human homolog, CXCL8), leading to (*3*) G-MDSC adhesion, diapedesis, and (*4*) Arg1- and iNOS-mediated lung vascular remodeling and PH.

Author disclosures are available with the text of this article at www.atsjournals.org.

Acknowledgments: The authors thank C. M. Eagan and J. West at the University of Florida for assistance with human studies, A. Fu for histologic preparation within the University of Florida Molecular and Pathology Core, M. Wallet and S. Wallet for technical support, and J. Fessel and J. West at Vanderbilt University for providing critical review of the manuscript.

References

1. Collard HR, Chen SY, Yeh WS, Li Q, Lee YC, Wang A, *et al*. Health care utilization and costs of idiopathic pulmonary fibrosis in U.S. Medicare beneficiaries aged 65 years and older. *Ann Am Thorac Soc* 2015;12: 981–987.
2. Collard HR, Ward AJ, Lanes S, Cortney Hayflinger D, Rosenberg DM, Hunsche E. Burden of illness in idiopathic pulmonary fibrosis. *J Med Econ* 2012;15:829–835.
3. Vaidya S, Hibbert CL, Kinter E, Boes S. Identification of key cost generating events for idiopathic pulmonary fibrosis: a systematic review. *Lung* 2017;195:1–8.
4. Lettieri CJ, Nathan SD, Barnett SD, Ahmad S, Shorr AF. Prevalence and outcomes of pulmonary arterial hypertension in advanced idiopathic pulmonary fibrosis. *Chest* 2006;129:746–752.
5. Nathan SD, Noble PW, Tuder RM. Idiopathic pulmonary fibrosis and pulmonary hypertension: connecting the dots. *Am J Respir Crit Care Med* 2007;175:875–880.
6. Bayer. Efficacy and safety of riociguat in patients with symptomatic pulmonary hypertension (PH) associated with idiopathic interstitial pneumonias (IIP) (RISE-IIP). 20170405. [Accessed 2017 Jul 20]. Available from: https://clinicaltrials.gov/ct2/show/NCT02138825.
7. Zisman DA, Schwarz M, Anstrom KJ, Collard HR, Flaherty KR, Hunninghake GW; Idiopathic Pulmonary Fibrosis Clinical Research Network. A controlled trial of sildenafil in advanced idiopathic pulmonary fibrosis. *N Engl J Med* 2010;363:620–628.
8. Raghu G, Behr J, Brown KK, Egan JJ, Kawut SM, Flaherty KR, *et al*.; ARTEMIS-IPF Investigators*. Treatment of idiopathic pulmonary fibrosis with ambrisentan: a parallel, randomized trial. *Ann Intern Med* 2013;158:641–649.
9. Bryant AJ, Carrick RP, McConaha ME, Jones BR, Shay SD, Moore CS, *et al*. Endothelial HIF signaling regulates pulmonary fibrosis–associated pulmonary hypertension. *Am J Physiol Lung Cell Mol Physiol* 2016;310: L249–L262.
10. Yan L, Chen X, Talati M, Nunley BW, Gladson S, Blackwell T, *et al*. Bone marrow–derived cells contribute to the pathogenesis of pulmonary arterial hypertension. *Am J Respir Crit Care Med* 2016;193:898–909.
11. Nagai H, Kuwahira I, Schwenke DO, Tsuchimochi H, Nara A, Ogura S, *et al*. Pulmonary macrophages attenuate hypoxic pulmonary vasoconstriction via β3AR/iNOS pathway in rats exposed to chronic intermittent hypoxia. *PLoS One* 2015;10:e0131923.
12. Tian W, Jiang X, Tamosiuniene R, Sung YK, Qian J, Dhillon G, *et al*. Blocking macrophage leukotriene B4 prevents endothelial injury and reverses pulmonary hypertension. *Sci Transl Med* 2013;5:200ra117.
13. Daley E, Emson C, Guignabert C, de Waal Malefyt R, Louten J, Kurup VP, *et al*. Pulmonary arterial remodeling induced by a Th2 immune response. *J Exp Med* 2008;205:361–372.
14. Hautefort A, Girerd B, Montani D, Cohen-Kaminsky S, Price L, Lambrecht BN, *et al*. T-helper 17 cell polarization in pulmonary arterial hypertension. *Chest* 2015;147:1610–1620.
15. Huertas A, Phan C, Bordenave J, Tu L, Thuillet R, Le Hiress M, *et al*. Regulatory T cell dysfunction in idiopathic, heritable and connective tissue-associated pulmonary arterial hypertension. *Chest* 2016;149:1482–1493.
16. Perros F, Cohen-Kaminsky S, Gambaryan N, Girerd B, Raymond N, Klingelschmitt I, *et al*. Cytotoxic cells and granulysin in pulmonary arterial hypertension and pulmonary veno-occlusive disease. *Am J Respir Crit Care Med* 2013;187:189–196.
17. Tamosiuniene R, Tian W, Dhillon G, Wang L, Sung YK, Gera L, *et al*. Regulatory T cells limit vascular endothelial injury and prevent pulmonary hypertension. *Circ Res* 2011;109:867–879.
18. Hoh BL, Hosaka K, Downes DP, Nowicki KW, Fernandez CE, Batich CD, *et al*. Monocyte chemotactic protein-1 promotes inflammatory vascular repair of murine carotid aneurysms via a macrophage inflammatory protein-1α and macrophage inflammatory protein-2–dependent pathway. *Circulation* 2011;124:2243–2252.
19. Burton VJ, Holmes AM, Ciuclan LI, Robinson A, Roger JS, Jarai G, *et al*. Attenuation of leukocyte recruitment via CXCR1/2 inhibition stops the progression of PAH in mice with genetic ablation of endothelial BMPR-II. *Blood* 2011;118:4750–4758.
20. Burton VJ, Ciuclan LI, Holmes AM, Rodman DM, Walker C, Budd DC. Bone morphogenetic protein receptor II regulates pulmonary artery endothelial cell barrier function. *Blood* 2011;117:333–341.
21. Russo RC, Guabiraba R, Garcia CC, Barcelos LS, Roffê E, Souza AL, *et al*. Role of the chemokine receptor CXCR2 in bleomycin-induced pulmonary inflammation and fibrosis. *Am J Respir Cell Mol Biol* 2009;40:410–421.
22. Condamine T, Kumar V, Ramachandran IR, Youn JI, Celis E, Finnberg N, *et al*. ER stress regulates myeloid-derived suppressor cell fate through TRAIL-R–mediated apoptosis. *J Clin Invest* 2014;124:2626–2639.
23. Murray LA, Chen Q, Kramer MS, Hesson DP, Argentieri RL, Peng X, *et al*. TGF-β driven lung fibrosis is macrophage dependent and blocked by serum amyloid P. *Int J Biochem Cell Biol* 2011;43:154–162.
24. Zaynagetdinov R, Sherrill TP, Kendall PL, Segal BH, Weller KP, Tighe RM, *et al*. Identification of myeloid cell subsets in murine lungs using flow cytometry. *Am J Respir Cell Mol Biol* 2013;49:180–189.
25. Baran CP, Opalek JM, McMaken S, Newland CA, O'Brien JM Jr, Hunter MG, *et al*. Important roles for macrophage colony–stimulating factor, CC chemokine ligand 2, and mononuclear phagocytes in the pathogenesis of pulmonary fibrosis. *Am J Respir Crit Care Med* 2007;176:78–89.
26. Bryant AJ, Robinson LJ, Moore CS, Blackwell TR, Gladson S, Penner NL, *et al*. Expression of mutant bone morphogenetic protein receptor II worsens pulmonary hypertension secondary to pulmonary fibrosis. *Pulm Circ* 2015;5:681–690.
27. Herz J, Sabellek P, Lane TE, Gunzer M, Hermann DM, Doeppner TR. Role of neutrophils in exacerbation of brain injury after focal cerebral ischemia in hyperlipidemic mice. *Stroke* 2015;46:2916–2925.
28. Lawson WE, Polosukhin VV, Stathopoulos GT, Zoia O, Han W, Lane KB, *et al*. Increased and prolonged pulmonary fibrosis in surfactant protein C–deficient mice following intratracheal bleomycin. *Am J Pathol* 2005; 167:1267–1277.
29. Lawson WE, Cheng DS, Degryse AL, Tanjore H, Polosukhin VV, Xu XC, *et al*. Endoplasmic reticulum stress enhances fibrotic remodeling in the lungs. *Proc Natl Acad Sci USA* 2011;108:10562–10567.
30. West J, Harral J, Lane K, Deng Y, Ickes B, Crona D, *et al*. Mice expressing BMPR2R899X transgene in smooth muscle develop pulmonary vascular lesions. *Am J Physiol Lung Cell Mol Physiol* 2008;295:L744–L755.
31. Hemnes AR, Brittain EL, Trammell AW, Fessel JP, Austin ED, Penner N, *et al*. Evidence for right ventricular lipotoxicity in heritable pulmonary arterial hypertension. *Am J Respir Crit Care Med* 2014; 189:325–334.
32. Degryse AL, Tanjore H, Xu XC, Polosukhin VV, Jones BR, Boomershine CS, *et al*. TGFβ signaling in lung epithelium regulates bleomycin-induced alveolar injury and fibroblast recruitment. *Am J Physiol Lung Cell Mol Physiol* 2011;300:L887–L897.
33. Tanjore H, Degryse AL, Crossno PF, Xu XC, McConaha ME, Jones BR, *et al*. β-catenin in the alveolar epithelium protects from lung fibrosis after intratracheal bleomycin. *Am J Respir Crit Care Med* 2013;187:630–639.
34. Karmouty-Quintana H, Zhong H, Acero L, Weng T, Melicoff E, West JD, *et al*. The A2B adenosine receptor modulates pulmonary hypertension associated with interstitial lung disease. *FASEB J* 2012; 26:2546–2557.
35. Hong KH, Lee YJ, Lee E, Park SO, Han C, Beppu H, *et al*. Genetic ablation of the BMPR2 gene in pulmonary endothelium is sufficient to predispose to pulmonary arterial hypertension. *Circulation* 2008;118:722–730.
36. Highfill SL, Cui Y, Giles AJ, Smith JP, Zhang H, Morse E, *et al*. Disruption of CXCR2-mediated MDSC tumor trafficking enhances anti-PD1 efficacy. *Sci Transl Med* 2014;6:237ra67.
37. Bryant AJ, Fu C, Brown GA, Biswas A, Shenoy V, Katovich M, *et al*. Macrophage depletion results in worsened secondary pulmonary hypertension and improved pulmonary fibrosis [abstract]. Presented

at the American Thoracic Society 2016 International Conference, May 13–18, 2016, San Francisco, CA. p. A7274.
38. King IL, Dickendesher TL, Segal BM. Circulating Ly-6C$^+$ myeloid precursors migrate to the CNS and play a pathogenic role during autoimmune demyelinating disease. *Blood* 2009;113:3190–3197.
39. Yee M, Buczynski BW, Lawrence BP, O'Reilly MA. Neonatal hyperoxia increases sensitivity of adult mice to bleomycin-induced lung fibrosis. *Am J Respir Cell Mol Biol* 2013;48:258–266.
40. Obregón-Henao A, Henao-Tamayo M, Orme IM, Ordway DJ. Gr1(int) CD11b$^+$ myeloid-derived suppressor cells in *Mycobacterium tuberculosis* infection. *PLoS One* 2013;8:e80669.
41. Ost M, Singh A, Peschel A, Mehling R, Rieber N, Hartl D. Myeloid-derived suppressor cells in bacterial infections. *Front Cell Infect Microbiol* 2016;6:37.
42. Fischer MA, Davies ML, Reider IE, Heipertz EL, Epler MR, Sei JJ, *et al*. CD11b$^+$, Ly6G$^+$ cells produce type I interferon and exhibit tissue protective properties following peripheral virus infection. *PLoS Pathog* 2011;7:e1002374.
43. Sharma SK, Chintala NK, Vadrevu SK, Patel J, Karbowniczek M, Markiewski MM. Pulmonary alveolar macrophages contribute to the premetastatic niche by suppressing antitumor T cell responses in the lungs. *J Immunol* 2015;194:5529–5538.
44. Bian Z, Guo Y, Ha B, Zen K, Liu Y. Regulation of the inflammatory response: enhancing neutrophil infiltration under chronic inflammatory conditions. *J Immunol* 2012;188:844–853.
45. Dyer DP, Pallas K, Ruiz LM, Schuette F, Wilson GJ, Graham GJ. CXCR2 deficient mice display macrophage-dependent exaggerated acute inflammatory responses. *Sci Rep* 2017;7:42681.
46. Highfill SL, Rodriguez PC, Zhou Q, Goetz CA, Koehn BH, Veenstra R, *et al*. Bone marrow myeloid–derived suppressor cells (MDSCs) inhibit graft-versus-host disease (GVHD) via an arginase-1–dependent mechanism that is up-regulated by interleukin-13. *Blood* 2010;116:5738–5747.
47. Frid MG, Brunetti JA, Burke DL, Carpenter TC, Davie NJ, Reeves JT, *et al*. Hypoxia-induced pulmonary vascular remodeling requires recruitment of circulating mesenchymal precursors of a monocyte/macrophage lineage. *Am J Pathol* 2006;168:659–669.
48. Thenappan T, Goel A, Marsboom G, Fang YH, Toth PT, Zhang HJ, *et al*. A central role for CD68(+) macrophages in hepatopulmonary syndrome: reversal by macrophage depletion. *Am J Respir Crit Care Med* 2011;183:1080–1091.
49. Gibbons MA, MacKinnon AC, Ramachandran P, Dhaliwal K, Duffin R, Phythian-Adams AT, *et al*. Ly6Chi monocytes direct alternatively activated profibrotic macrophage regulation of lung fibrosis. *Am J Respir Crit Care Med* 2011;184:569–581.
50. Du R, Lu KV, Petritsch C, Liu P, Ganss R, Passegué E, *et al*. HIF1α induces the recruitment of bone marrow–derived vascular modulatory cells to regulate tumor angiogenesis and invasion. *Cancer Cell* 2008;13:206–220.
51. Grimshaw MJ, Wilson JL, Balkwill FR. Endothelin-2 is a macrophage chemoattractant: implications for macrophage distribution in tumors. *Eur J Immunol* 2002;32:2393–2400.
52. Meyrick B, Reid L. The effect of continued hypoxia on rat pulmonary arterial circulation: an ultrastructural study. *Lab Invest* 1978;38: 188–200.
53. Carré PC, Mortenson RL, King TE Jr, Noble PW, Sable CL, Riches DW. Increased expression of the interleukin-8 gene by alveolar macrophages in idiopathic pulmonary fibrosis: a potential mechanism for the recruitment and activation of neutrophils in lung fibrosis. *J Clin Invest* 1991;88:1802–1810.
54. Droma Y, Hayano T, Takabayashi Y, Koizumi T, Kubo K, Kobayashi T, *et al*. Endothelin-1 and interleukin-8 in high altitude pulmonary oedema. *Eur Respir J* 1996;9:1947–1949.
55. Giordano S, Zhao X, Xing D, Hage F, Oparil S, Cooke JP, *et al*. Targeted delivery of human iPS-ECs overexpressing IL-8 receptors inhibits neointimal and inflammatory responses to vascular injury in the rat. *Am J Physiol Heart Circ Physiol* 2016;310:H705–H715.
56. Lee AH, Dhaliwal R, Kantores C, Ivanovska J, Gosal K, McNamara PJ, *et al*. Rho-kinase inhibitor prevents bleomycin-induced injury in neonatal rats independent of effects on lung inflammation. *Am J Respir Cell Mol Biol* 2014;50:61–73.
57. Bronte V, Brandau S, Chen SH, Colombo MP, Frey AB, Greten TF, *et al*. Recommendations for myeloid-derived suppressor cell nomenclature and characterization standards. *Nat Commun* 2016;7:12150.
58. Gabrilovich DI. Myeloid-derived suppressor cells. *Cancer Immunol Res* 2017;5:3–8.
59. Lin S, Wang J, Wang L, Wen J, Guo Y, Qiao W, *et al*. Phosphodiesterase-5 inhibition suppresses colonic inflammation-induced tumorigenesis via blocking the recruitment of MDSC. *Am J Cancer Res* 2017;7: 41–52.
60. Martire-Greco D, Rodriguez-Rodrigues N, Castillo LA, Vecchione MB, de Campos-Nebel M, Córdoba Moreno M, *et al*. Novel use of all-trans-retinoic acid in a model of lipopolysaccharide-immunosuppression to decrease the generation of myeloid-derived suppressor cells by reducing the proliferation of CD34$^+$ precursor cells. *Shock* 2017;48:94–103.
61. Draghiciu O, Nijman HW, Hoogeboom BN, Meijerhof T, Daemen T. Sunitinib depletes myeloid-derived suppressor cells and synergizes with a cancer vaccine to enhance antigen-specific immune responses and tumor eradication. *OncoImmunology* 2015;4:e989764.
62. Rennard SI, Dale DC, Donohue JF, Kanniess F, Magnussen H, Sutherland ER, *et al*. CXCR2 antagonist MK-7123: a phase 2 proof-of-concept trial for chronic obstructive pulmonary disease. *Am J Respir Crit Care Med* 2015;191:1001–1011.
63. Yeager ME, Nguyen CM, Belchenko DD, Colvin KL, Takatsuki S, Ivy DD, *et al*. Circulating myeloid-derived suppressor cells are increased and activated in pulmonary hypertension. *Chest* 2012;141:944–952.
64. Fernandez IE, Greiffo FR, Frankenberger M, Bandres J, Heinzelmann K, Neurohr C, *et al*. Peripheral blood myeloid-derived suppressor cells reflect disease status in idiopathic pulmonary fibrosis. *Eur Respir J* 2016;48:1171–1183.
65. Bronte V, Zanovello P. Regulation of immune responses by L-arginine metabolism. *Nat Rev Immunol* 2005;5:641–654.
66. Rodriguez PC, Ernstoff MS, Hernandez C, Atkins M, Zabaleta J, Sierra R, *et al*. Arginase I–producing myeloid-derived suppressor cells in renal cell carcinoma are a subpopulation of activated granulocytes. *Cancer Res* 2009;69:1553–1560.
67. Koehn BH, Apostolova P, Haverkamp JM, Miller JS, McCullar V, Tolar J, *et al*. GVHD-associated, inflammasome-mediated loss of function in adoptively transferred myeloid-derived suppressor cells. *Blood* 2015;126:1621–1628.
68. Marigo I, Bosio E, Solito S, Mesa C, Fernandez A, Dolcetti L, *et al*. Tumor-induced tolerance and immune suppression depend on the C/EBPβ transcription factor. *Immunity* 2010;32:790–802.
69. Amsellem V, Abid S, Poupel L, Parpaleix A, Rodero M, Gary-Bobo G, *et al*. Roles for the CX3CL1/CX3CR1 and CCL2/CCR2 chemokine systems in hypoxic pulmonary hypertension. *Am J Respir Cell Mol Biol* 2017;56:597–608.
70. Talati M, West J, Zaynagetdinov R, Hong CC, Han W, Blackwell T, *et al*. BMP pathway regulation of and by macrophages. *PLoS One* 2014;9:e94119.
71. Vergadi E, Chang MS, Lee C, Liang OD, Liu X, Fernandez-Gonzalez A, *et al*. Early macrophage recruitment and alternative activation are critical for the later development of hypoxia-induced pulmonary hypertension. *Circulation* 2011;123:1986–1995.
72. Johnson DB, Balko JM, Compton ML, Chalkias S, Gorham J, Xu Y, *et al*. Fulminant myocarditis with combination immune checkpoint blockade. *N Engl J Med* 2016;375:1749–1755.